Location of Agricultural Drainage Pipes and Assessment of Agricultural Drainage Pipe Conditions Using Ground Penetrating Radar

Barry J. Allred[1] and J. David Redman[2]
[1]USDA/ARS – Soil Drainage Research Unit, 590 Woody Hayes Drive, Room 234, Columbus, Oh., USA, 43210
Email: barry.allred@ars.usda.gov
[2]Sensors & Software Inc., 1040 Stacey Court, Mississuaga, Ont., L4W 2X8, Canada

ABSTRACT

Methods are needed to not only locate buried agricultural drainage pipe, but to also determine if the pipes are functioning properly with respect to water delivery. The primary focus of this research project was to confirm the ability of ground penetrating radar (GPR) to locate buried drainage pipe, and then determine if GPR provides insight into drain line water conveyance functionality. Ground penetrating radar surveys using 250 MHz transmitter/receiver antennas were conducted at a specially designed test plot under drained, moderately wet soil conditions (water table below drain lines) and undrained, extremely wet soil conditions (water table above drain lines). The test plot contained four drain lines: one a clay tile to corrugated plastic tubing (CPT) drain line that was completely open to flow; one comprised of CPT with an isolated obstruction near the midpoint, completely preventing through-flow of water; one comprised of CPT but filled with soil; and one comprised of CPT but severed near its midpoint, producing a partial obstruction to water flow. Subsequent GPR computer modeling simulations were employed to assist with interpretation of the GPR field data. Results of the GPR field surveys indicate that given suitable shallow hydrologic conditions, GPR not only finds drainage pipes, but can also determine the position along a drain line where there is an isolated obstruction that completely blocks water flow. However, results show that a partial pipe obstruction is difficult to locate using GPR. Surprisingly, the soil-filled drain line was clearly detectable under both soil hydrologic conditions tested. The GPR computer modeling simulations indicate that soil had likely settled within the pipe, and that the GPR responses obtained at the test plot for the soil-filled pipe were responses representative of a pipe that was in fact only partially filled with soil. Overall, these research results provide valuable information for those contemplating the use of GPR to locate agricultural drainage pipes and then determine their functionality.

Introduction

A 1985 economic survey (Pavelis, 1987) showed that the states comprising the Midwest U.S. (Illinois, Indiana, Iowa, Ohio, Minnesota, Michigan, Missouri, and Wisconsin) had by that year approximately 12.5 million hectares that contained subsurface drainage systems. Cropland accounts for the large majority of the Midwest U.S. areas that have these buried drainage pipe networks. Farmers within this region often need to improve or repair pre-existing subsurface drainage pipe systems, but before this is done, drain lines have to be located and then a determination made as to whether they are functioning properly. Several investigations have documented the capability of ground penetrating radar (GPR) to find buried plastic or metal utility pipelines (LaFaleche *et al.*, 1991; Wensink *et al.*, 1991; Zeng and McMechan, 1997; Hayakawa and Kawanaka, 1998). The ElectroScience Laboratory at Ohio State University developed a GPR system capable of finding 60% of plastic utility pipes in 60% of the U.S. (Peters and Young, 1986). There has also been prior research specifically indicating that GPR can be effective in locating buried drainage pipes. Chow and Rees (1989) demonstrated the use of GPR to locate subsurface agricultural drainage pipes in the Maritime Provinces of Canada, while Boniak *et al.* (2002) and Allred *et al.* (2005a) showed that GPR could be employed to find drainage pipe beneath golf course greens and tees. Ground penetrating radar surveys were conducted in southwest, central, and northwest Ohio at fourteen test plots (including the one used in this study), and with respect to locating the total amount of pipe present at each site, this technology was shown to have an average effectiveness of 74%; with 100% of the pipe found at seven sites, 90% at one site, 75% at two sites, 50% at two sites, and 0% at two sites (Allred *et al.*, 2004; Allred *et al.*, 2005b). Based on this testing conducted in Ohio, GPR was shown to be reasonably successful in finding clay tile and corrugated plastic tubing (CPT) drainage pipe down to depths of around 1 m in a variety of different soil types. Allred *et al.* (2005b) additionally determined the impact of computer processing procedures, equipment attributes, site conditions, and field operations on GPR drainage pipe detection.

These previous investigations clearly indicate the feasibility of using GPR to locate buried agricultural drainage pipes. However, to date, there has been very little research on determining if GPR can provide insight into whether a drain line is functioning properly. Differential compaction from farm equipment operations, uneven settlement, and deep tillage practices can potentially cause pipe severing or collapse at a point along a drain line. Drainage pipe severing or collapse can produce a partial or complete obstruction to water flow through the drain line, in turn resulting in crop damage caused by inadequate soil water drainage in an area adjacent to the portion of the drain line up-gradient of the pipe obstruction. Furthermore, in Ohio and many other Midwest U.S. locations, the typical practice is to not place filter material around the drain lines during installation. This practice reduces cost, but occasionally causes problems when fine-grained soil materials enter a drainage pipe through joints or perforations (Fig. 1). If the build-up of soil material within the drainage pipe becomes excessive, drain line water flow becomes restricted. Due to the causes described, drainage pipe failures and their consequences are not uncommon. Therefore, effective and efficient methods are needed to gauge drain line functionality, and in this regard, GPR may provide the solution.

The primary objective of this research project was to confirm GPR drainage pipe detection capabilities and then evaluate whether GPR is capable of determining drainage pipe conditions with respect to water conveyance functionality. To accomplish the research objective, GPR was tested under drained, moderately wet and undrained, extremely wet soil conditions at a specially designed test plot containing an open, totally unobstructed drain line; a completely obstructed drain line, plugged near its midpoint; a soil-filled drain line; and a severed, partially obstructed drain line. Ground penetrating radar computer modeling simulations assisted with interpretation of GPR data obtained at the test plot. The guiding research hypothesis is stated as follows, "Given a suitable set of circumstances with respect to shallow hydrology, ground penetrating radar will not only locate drainage pipes, but can also provide useful insight on conditions affecting the flow of water within the drainage pipes."

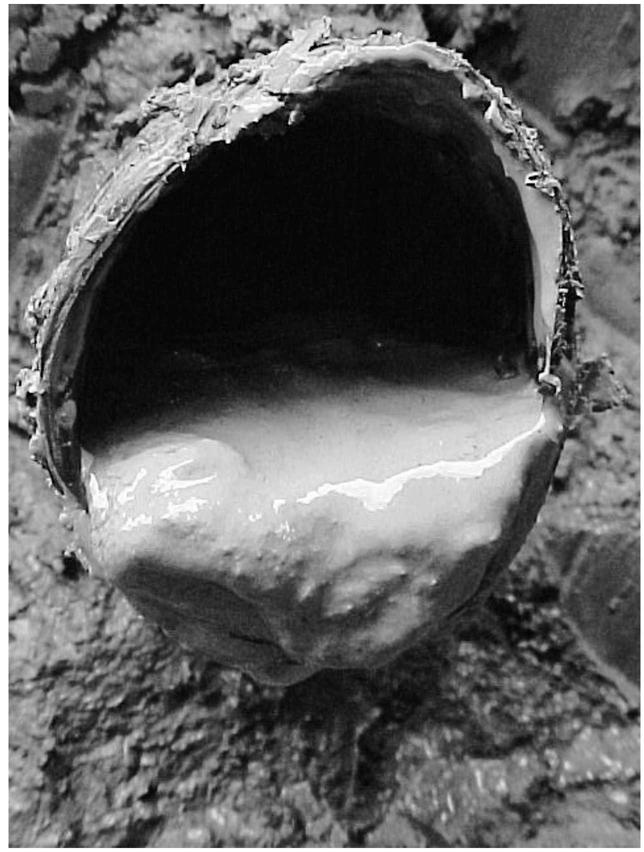

Figure 1. Agricultural drainage pipe partially filled with sediment.

Methodology

<u>Test Plot Description</u>

A test plot specifically designed for this project was constructed in late July 2006. Four drain lines were installed at a 12.2 m east-west by 24.4 m north-south test plot located at the Ohio State University - Waterman Agricultural and Natural Resources Laboratory in Columbus, Ohio. Figures 2(a) and 2(b) are schematic profiles of an installed drain line. Trenching equipment was used to install the drain lines. Once four trenches were excavated, a drain line was placed at the bottom of each trench, and the trenches were then backfilled with the excavated soil material. Afterwards, the entire test plot was tilled to a depth of 0.3 m. Following tillage, a grass cover was allowed to develop across the test plot. The installed drainage pipe had an inside diameter of 0.10 m and an outside diameter of 0.12 m. (Note:

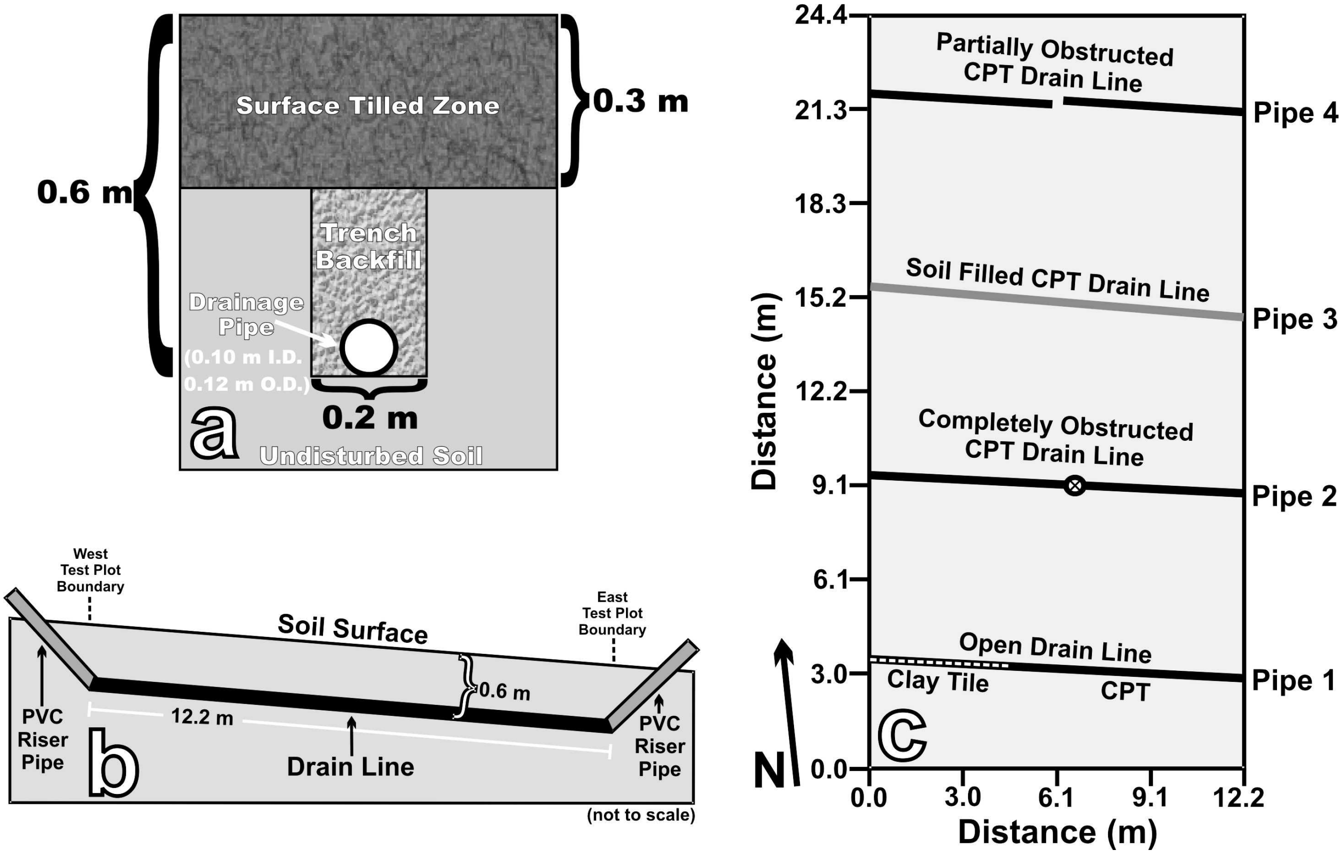

Figure 2. Test plot schematics: (a) profile oriented perpendicular to drainage pipe direction, (b) profile along the length of a drain line, (c) map showing locations for installed drain lines.

Because of the corrugations, the corrugated plastic tubing drainage pipe that was used had a minimum inside diameter of 0.10 m and a maximum outside diameter of 0.12 m, even though the wall thickness is only 0.001 m. Clay tile drainage pipe used had a wall thickness of 0.01 m, a consistent inside diameter of 0.10 m, and a consistent outside diameter of 0.12 m.) Each drain line had a length of 12.2 m. The backfilled trenches had a width of 0.2 m and a depth of approximately 0.6 m.

Within typical Ohio agricultural settings, the tilled zone thickness is 0.3 m or less, and the trench where a drainage pipe is placed usually has a width between 0.2 to 0.5 m. Although somewhat shallow, the test plot trench depth is within range of the depths that drainage pipe in Ohio are typically buried (0.5 to 1.0 m). Deeper trenches were not excavated because the research focus was on obtaining the best quality GPR data possible to evaluate feasibility of assessing drainage pipe condition. Polyvinyl chloride (PVC) riser pipe (0.10 m inside diameter) were extended from both ends of a drain line to a height of 0.3 m above the ground surface, thereby allowing water to be easily added or removed from a drain line (Fig. 2(b)). The soil surface and the drain line itself slope downwards approximately 0.2 m from the west to east ends of a drain line.

A schematic map of the test plot showing drain line locations is provided in Fig. 2(c). The southernmost drain line is, for simplicity, designated Pipe 1 and is comprised, from west to east, of 4.2 m of clay tile pipe and then 8.0 m of CPT. Pipe 1 has no obstructions, allowing the free flow of water along its length. The next drain line to the north is Pipe 2. This CPT drain line was severed near its center at a position 5.5 m from the east test plot boundary. The severed ends within Pipe 2 were then capped and realigned with one another to produce an isolated obstruction completely blocking water flow. Pipe 3 is directly north of Pipe 2. Pipe 3 is comprised of a CPT drain line that was filled with soil excavated during installation. The northern most drain line, designated as Pipe 4, is comprised of CPT and is severed at its midpoint. The uncapped severed ends within Pipe 4 were offset from one another, but still overlapped, thereby producing both a partial obstruction to flow and a location where significant quantities of water could potentially leak out of the drain line.

The soil covering the test plot is derived from glacial till and is part of the Crosby Series (fine, mixed, mesic Aeric Ochraqualfs). Four soil samples were obtained at the test plot, one from each of the backfilled trenches where new drain lines had been placed. Every sample was comprised of a mixture of soil from along the length of one of the four excavated trenches and includes material from the surface to a depth of 0.6 m. A particle size analysis (Wray, 1986) was conducted on each soil sample, and the results were quite consistent, with a percent sand range of 21.9% to 25.1%, a percent silt range of 44.9% to 46.6%, and a percent clay range of 29.5% to 31.6%. All four soil samples are classified as a clay loam, which indicates that soil texture changed very little across the test plot. Test plot topography was mapped with real-time kinematic (RTK) global positioning system (GPS) technology using a Topcon Positioning Systems, Inc. (Livermore California), HiPer XT Wireless RTK GPS. The ground surface of the test plot slopes downward in a fairly uniform manner from the southwest corner to the northeast corner. The total elevation difference between the southwest and northeast corners is 0.55 m.

Test Plot Preparation

Field data were collected during two time periods. The first data collection period was October 15–16, 2006. A sprinkler irrigation system was used to apply water to the test plot surface during September 26–28, 2006 in order to completely saturate the soil profile. The test plot was then allowed to drain over the next sixteen days. During these sixteen days there were only two modest rainfall events, so by October 15, 2006, the test plot conditions were drained (water table below drain lines, air- or unsaturated soil-filled pipes), but with the soil profile still moderately wet. A 3.5-m long, 0.02-m diameter flexible PVC pipe with its outside surface coated with water-indicating paste (Kolor Kut Water Finding Paste, Kolor Kut Products Company, Houston, Texas) was inserted into the PVC riser pipe at both ends of each drain line to confirm that the drain lines were either air-filled (Pipes 1, 2, and 4) or contained unsaturated soil (Pipe 3). Given properly functioning drain lines, these October 15–16, 2006 test plot conditions are common throughout Ohio during late fall, winter, and early spring, a few days after a major rainfall event.

After field data were collected on October 15–16, 2006, sprinkler irrigation was again used to apply water to the test plot surface beginning shortly after 12:00 noon on October 16, 2006. Sprinkler irrigation was discontinued approximately 12 h later, when heavy rainfall began and it was concluded that applying additional water was no longer necessary. Heavy, intermittent rainfall continued until the morning of October 20, 2006. Consequently, test plot conditions during the second field data collection period, Oct. 19–20, 2006, were undrained (water table above drain lines, water- or saturated soil-filled pipes) with an extremely wet soil profile and a few isolated locations where there was water ponding in shallow surface depressions. Again, a 3.5-m long, 0.02-m diameter flexible PVC pipe with its outside surface coated with water-indicating paste was inserted into the PVC riser pipe at both ends of each drain line to confirm that the drain lines were either water-filled (Pipes 1, 2, and 4) or contained saturated soil (Pipe 3). These October 19–20, 2006 test plot conditions are common throughout Ohio in the late fall, winter, and early spring months, during or very shortly after a prolonged rainfall event.

Ground Penetrating Radar Equipment and Equipment Settings

A Sensors & Software Inc. (Mississuaga, Ontario, Canada), Noggin^{plus} GPR unit with 250 MHz antennas and an integrated odometer was used to study GPR drainage pipe responses. The Noggin^{plus} GPR unit with 250 MHz center frequency antennas was chosen for use in this study because of its drainage pipe detection success in previous investigations (Allred *et al.*, 2004; Allred *et al.*, 2005a; Allred *et al.*, 2005b). For this GPR unit, the separation distance between the 250 MHz transmitter and receiver antennas is 0.28 m. This antenna separation distance is optimal for minimizing attenuation losses and maximizing target coupling and system dynamic range. The antennas themselves were always oriented perpendicular to the measurement transects along which data were collected. In addition, this GPR system was set-up to have a 0.05-m separation distance between measurement points on a transect, and 32 signal traces were averaged (stacked) at each measurement point, with a 0.4-ns sampling interval along each signal trace.

Ground Penetrating Radar Test Plot Data Collection

Two GPR data sets were collected, one for each shallow hydrologic condition (drained, moderately wet and undrained, extremely wet). For both shallow hydrologic conditions, GPR measurements were first obtained along a series of south-to-north transects beginning with the west test plot boundary and finishing with the east test plot boundary. All eleven south-to-north GPR measurement lines in a series were 24.4 m in length, spaced 1.2 m apart, started at the south test plot boundary, and ended at the north test plot boundary. While this 1.2-m spacing distance between south-to-north measurement transects does not provide complete GPR spatial coverage within the test plot to detect small isolated targets, it is more than adequate for GPR imaging of drain lines that extend from west to east across the test plot (drainage pipes essentially trend perpendicular to the orientation of the south-to-north GPR measurement transects). The grid of south-north measurement transects used to collect GPR data were staked out on the test plot with measuring tapes. Following GPR data collection along a particular series of south-to-north transects, GPR data were additionally obtained along four 12.2 m west-to-east transects oriented directly over top and along trend with the four recently installed test plot drain lines. Two supplementary west-to-east GPR transects were obtained under undrained, extremely wet conditions for Pipes 2 and 4 while water was being pumped out of the east ends of both drain lines. Locations for individual GPR measurements along any particular transect were determined with a highly accurate and precise odometer, which is an integrated component of the Noggin^{plus} GPR unit.

Ground Penetrating Radar Test Plot Data Processing

GPR time/depth profiles showing drainage pipe responses were generated for each south-to-north or west-to-east measurement transect along which GPR data were collected. Computer processing of the GPR profiles required application of a signal saturation correction filter to remove low frequency noise, followed by signal amplification, which was accomplished using a spreading and exponential compensation gain function having a start value of 1.0, an attenuation of 7.5 decibels/m, and a maximum gain factor of 250. Two GPR amplitude maps were also produced, one for each shallow hydrologic condition. To generate a GPR amplitude map for a particular shallow hydrologic condition, data were used from the corresponding series of eleven south-to-north GPR transects. On these maps, drainage pipes appear as high amplitude, lighter shaded linear features. The computer processing steps used to produce the GPR amplitude maps for this project included: a signal saturation correction filter, signal trace enveloping, 2-D migration, and a spatial background subtraction filter. Signal trace enveloping converts signal wavelets having positive and negative components into ones that are unipolar and positive, thereby removing the oscillatory nature of radar signal wavelets (Sensors & Software Inc., 2003). Or, described in another way, the signal trace enveloping process makes all the negative components of a radar signal wavelet positive and then smoothes the wavelet outline. The 2-D migration step collapses hyperbolic responses to point targets. The spatial background subtraction filter suppressed flat-lying features.

Electromagnetic Induction and Time Domain Reflectometry Equipment and Test Plot Data Collection

Apparent soil electrical conductivity (EC_a) test plot conditions were measured by employing the electromagnetic induction method with a Geophex, Ltd. (Raleigh, North Carolina), GEM-2 ground conductivity meter operated at a frequency of 14.6 kHz, with approximately ten measurements taken per second. The co-planer transmitter/receiver intercoil spacing, s, is 1.66 m, and during use the GEM-2 was held approximately 1-m above the ground surface and oriented in the vertical dipole mode (horizontal co-planer coil configuration). Test plot volumetric water content values near the soil surface were measured using a Spectrum Technologies, Inc. (East Plainfield, Illinois), Field Scout TDR-300. The Field Scout TDR-300 employs a time domain reflectometry (TDR) approach to determine the average volumetric water content from the surface to a depth of 0.2 m at each point location a measurement is taken.

Measurements of apparent soil electrical conductivity (EC_a) and near surface soil volumetric water content (0.0 to 0.2 m depth) were obtained along with the GPR measurements during the two data collection periods. Electromagnetic induction EC_a measurements were collected on October 16, 2006 and October 20, 2006 with the GEM-2 along the same south-north transects that GPR data were obtained. The GEM-2 equipment design compensates for internal temperature change, and periodic electromagnetic induction readings obtained when a ferrite rod was placed on the GEM-2 at a specified location ensured that the GEM-2 remained calibrated and did not require calibration adjustment. The average and standard deviation values of test plot EC_a were then computed for both shallow hydrologic conditions. Near surface soil volumetric water content was measured with the Field Scout TDR-300 at twenty-one evenly spaced test plot locations on October 16, 2006 and October 20, 2006. The twenty-one soil volumetric water content measurements for a data collection event were in turn used to compute average and standard deviation values that were then employed to evaluate the water content changes that occurred as test plot shallow hydrologic conditions went from drained, moderately wet to undrained, extremely wet.

Ground Penetrating Radar Computer Modeling

Finite difference, time domain, three-dimensional (3-D) GPR computer modeling software, GprMax3D (Giannopoulos, 2009), was utilized to generate synthetic GPR profiles depicting drainage pipe responses. As a preliminary step, two-dimensional (2-D) GPR modeling software, GprMax2D (Giannopoulos, 2009) was used to provide sufficient spatial resolution of the pipe wall.

Computer simulation using GprMax2D demonstrated that the pipe wall, which is relatively thin, has minor effect on the drainage pipe response. In fact, the GPR response for plastic and clay tile pipes, as depicted on GPR profiles, is controlled principally by the contrast in relative dielectric permittivity between the material contained within the pipe (air, water, or soil) and the surrounding soil (Zeng and McMechan, 1997). Further confirmation of this assertion is provided in a field investigation conducted by Allred *et al.* (2005b), which found that the type of material comprising the drainage pipe, either corrugated plastic tubing (CPT) or clay tile, has no effect on the GPR drainage pipe response. These findings are a result of the drainage pipe wall thickness being small compared to the wavelength of the radar signal. The bandwidth of the 250 MHz Noggin^{plus} GPR unit is ~250 MHz, so the antenna frequency range is approximately 250 MHz ± 125 MHz. Based on this frequency range, the radar wavelengths in moderately wet to extremely wet clay loam soils present at the test plot range approximately between 0.7 m to 0.15 m. Drainage pipe wall thickness is approximately 0.001 m for CPT pipe and 0.01 m for clay tile pipe. Both of these drainage pipe thicknesses are much smaller than the range of radar wavelengths (0.7 m to 0.15 m) transmitted through moderately wet to extremely wet clay loam soils by the 250 MHz Noggin^{plus} GPR unit.

Three-dimensional computer modeling with GprMax3D, which is more computationally demanding than 2-D modeling with GPRMax2D, was required to simulate the case of the antennas oriented perpendicular to the drain line and to also provide synthetic GPR profiles with more accurate radar signal amplitudes. Since the higher spatial resolution 2-D GPR modeling with GprMax2D proved that the drainage pipe wall has minor effect on the GPR response, the pipe wall input therefore was omitted from the GprMax3D 3-D modeling to allow for a larger cell size and reduced computational demands needed to generate the GPR profiles. GprMax3D was used to generate synthetic profiles showing GPR pipe responses for scenarios with various combinations of moderately wet or extremely wet soil surrounding the pipe; air, water, or soil contained within the pipe; and a measurement transect direction either perpendicular to the pipe (antennas oriented parallel to the pipe) or over top and along trend of the pipe (antennas oriented perpendicular to the pipe). Modeling parameters included a 0.28-m separation distance between transmitter and receiver antennas, a source signal comprised of a standard Ricker wavelet with a 250 MHz center frequency, and a distance between transect measurement points set at 0.05 m. These modeling parameters were chosen to coincide with the GPR equipment characteristics and settings used for field data acquisition. In addition, radar signal was amplified for the synthetic GPR profiles by employing a constant gain factor of 20. The synthetic GPR profiles were used to help interpret the GPR profiles produced from data actually collected at the test plot.

Results and Discussion

Apparent Soil Electrical Conductivity (EC_a), Soil Volumetric Water Content, Soil Relative Dielectric Permittivity, and Soil Radar Velocity Test Plot Data

Test plot average and standard deviation values for apparent soil electrical conductivity (measured with electromagnetic induction methods), near surface soil volumetric water content (determined by time domain reflectometry), and soil relative dielectric permittivity (calculated from volumetric water content), are provided in Table 1. Observations on October 16, 2006 that the water table was below the four recently installed drain lines, combined with an average near surface soil volumetric water content of 27.9% on that date, indicates that the test plot soil profile hydrologic conditions were drained and moderately wet during the October 15–16, 2006 field data collection period. The average near surface soil volumetric water content on October 20, 2006 was 35.0%, which along with observations that the water table was above the four recently installed drain lines, indicates that the test plot soil profile hydrologic conditions were undrained and extremely wet during the October 19–20, 2006 field data collection period. The average and standard deviation values for the soil relative dielectric permittivity under drained, moderately wet soil conditions and undrained, extremely wet soil conditions were calculated using the test plot soil volumetric water content measurements and an empirical equation developed by Sutinen (1992) for glacially derived soil materials. Table 1 shows that as test plot shallow hydrologic conditions went from drained, moderately wet to undrained, extremely wet, the soil relative dielectric permittivity increased, on average, from 19.7 to 25.4. A relative dielectric permittivity of 19.7 corresponds to a soil radar velocity of 0.0675 m/ns, while a relative dielectric permittivity of 25.4 corresponds to a radar velocity of 0.0595 m/ns (Conyers, 2004). These radar velocities, 0.0675 m/ns for drained, moderately wet soil and 0.0595 m/ns for undrained, extremely wet soil, were employed to convert two-way radar signal travel time to depth values. It should be noted that modeled hyperbolic curves were fitted to GPR drainage pipe reflection hyperbola responses to confirm the accuracy of the drained, moderately wet and undrained, extremely wet soil radar velocities, and hence the drained, moderately wet and

Table 1. Average and standard deviation (in parenthesis) of test plot soil condition measurements.

Data collection date	Soil volumetric water content (%)	Soil relative dielectric permittivity (dimensionless)	Apparent soil electrical conductivity (EC_a) (mS/m)
October 16, 2006	27.9 (±3.4)	19.7 (±2.6)	14.7 (±2.5)
October 20, 2006	35.0 (±3.5)	25.4 (±2.9)	17.7 (±2.4)

undrained, extremely wet soil relative dielectric permittivities that were determined from TDR water content measurements and the empirical equation developed by Sutinen (1992). The average and standard deviation values for test plot apparent soil electrical conductivity (EC_a) given in Table 1 are relatively small, 14.7 ± 2.5 mS/m under drained, moderately wet conditions, and 17.7 ± 2.4 mS/m under undrained, extremely wet conditions. Consequently, regardless of the shallow hydrologic conditions present, the uniformly low EC_a values found across the test plot imply that radar signal attenuation was not a major factor of concern with respect to GPR imaging of drainage pipes positioned approximately 0.6 m beneath the ground surface. These EC_a values along with the soil relative dielectric permittivity values were also used as input parameters for the GPR computer modeling simulations.

Ground Penetrating Radar Test Plot Data

During wet periods of the year, after a large rainfall event, and given a properly functioning drain line, the up-gradient, higher elevation portions of a drain line will drain first and become air-filled, while the down-gradient, lower elevation portions of the drain line are still water-filled. When an obstruction to water flow is present within the drain line, a reversed situation may prevail after a large rainfall event. Consequently, if GPR methods are capable of accurately determining whether a drainage pipe is air- or water-filled, then given the proper shallow hydrologic conditions, GPR could be employed to indicate whether there is an obstruction along a drain line that inhibits the flow of water. Specifically, a GPR finding that up-gradient, higher elevation portions of the drain line remain water-filled, while down-gradient, lower elevation portions of the drain line are air-filled, is a clear indication that an obstruction to water flow exists along the drain line. Water flow obstructions along a drain line may be isolated at a single point, where for example a drainage pipe has collapsed or been severed. Alternatively, sedimentation inside a drain line can produce long segments of drainage pipe that become plugged with soil, also inhibiting water flow. Therefore, if GPR can distinguish between an air-filled drainage pipe versus a water-filled drainage pipe versus a soil-filled drainage pipe, then given the right circumstances, not only can the presence of a drain line water flow obstruction be deduced, but information on the nature of the obstruction could additionally be ascertained.

Figure 3 displays GPR results from data collected from two series of eleven south-to-north measurement transects (one series for drained, moderately wet soil conditions and the second series for undrained, extremely wet soil conditions). Each GPR amplitude map (Figs. 3(a) and 3(c)) was generated with respect to the shortest two-way radar signal travel-time interval that encompassed all GPR drainage pipe responses. Consequently, the Fig. 3(a) GPR amplitude map represents a 14- to 25-ns two-way travel-time interval, while the Fig. 3(c) GPR amplitude map represents a larger 14- to 30-ns two-way travel-time interval. The drain lines are labeled and show up as lighter-shaded linear features on the GPR amplitude maps.

The Fig. 3(a) and Fig. 3(c) GPR amplitude maps depict one of the more unexpected findings of this study, which is the presence of two older test plot drain lines, Pipe A and Pipe B, that were not previously known to exist. There is no information available on Pipe A and Pipe B as to when they were put in place, the material of which they are comprised, or whether they are a part of a much larger subsurface drainage system that is still functioning. Although all drain lines (Pipes 1, 2, 3, 4, A, and B) show up fairly well in both the GPR amplitude maps, they are somewhat clearer in Fig. 3(a) compared to Fig. 3(c), supporting previous research by Allred *et al.* (2005b) indicating that drained, moderately wet conditions are better than undrained, extremely wet conditions for mapping subsurface drainage systems. Perhaps the most important aspect of Figs. 3(a) and 3(c), when they are viewed individually, is that the mapped GPR response for the soil-filled Pipe 3 is generally weaker than the mapped GPR response for Pipes 1, 2, and 4. Therefore, a weak response exhibited on a GPR amplitude map for a particular drain line when compared to other drain lines shown on the GPR amplitude map could potentially indicate that the drain line with the weaker response is substantially soil-filled.

Figures 3(b) and 3(d) are representative south-to-north GPR time/depth profiles generated from data collected along a measurement transect located 2.4-m

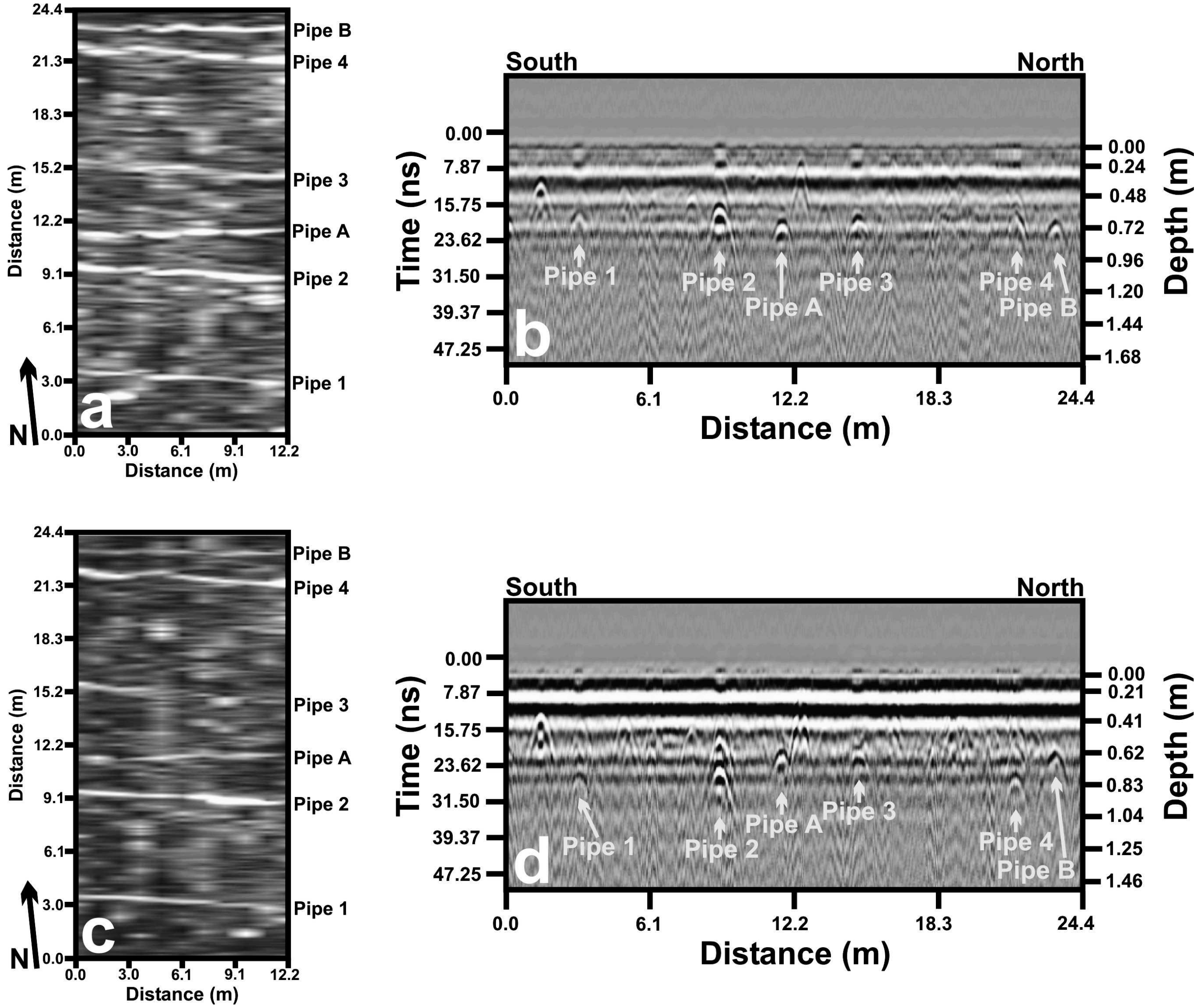

Figure 3. GPR results from data collected along two series of south-to-north transects in which each series was collected under different shallow hydrologic conditions: (a) GPR amplitude map from drained, moderately wet conditions based on a time interval of 14 to 25 ns, (b) south-to north GPR profile representing drained, moderately wet conditions, (c) GPR amplitude map from undrained, extremely wet conditions based on a time interval of 14 to 30 ns, and (d) south-to-north GPR profile representing undrained, extremely wet conditions.

west of the east test plot boundary. The test plot drain lines are essentially perpendicular to the south-to-north measurement transect along which data for the Figs. 3(b) and 3(d) GPR profiles were collected. With the drain lines and the measurement transect oriented perpendicular to one another, the GPR drainage pipe response shown in the Figs. 3(b) and 3(d) profiles is that of one or two inverted U-shaped features, commonly referred to as reflection hyperbolas. The reflection hyperbola apex provides information on drain line depth and its distance position along the GPR profile measurement transect. Labels are provided in Figs. 3(b) and 3(d) for all six drain line reflection hyperbola responses. Figures 3(b) and 3(d) also show an additional strong reflection hyperbola response (unlabeled) that is directly south of the Pipe 1 reflection hyperbola. This particular reflection hyperbola represents an isolated feature of unknown origin that was not detected on other south-to-north GPR profiles.

Under drained, moderately wet conditions with air- or unsaturated soil-filled pipes, each drain line visible on south-to-north GPR profiles, such as Fig. 3(b), is represented by a single clearly distinguishable reflection hyperbola response. Under undrained, extremely wet conditions, individual water-filled drain lines visible on south-to-north GPR profiles, such as Fig. 3(d), were often represented by upper and lower reflection hyperbolas. The presence of upper and lower reflection hyperbolas representing individual pipes is what necessitated the use of a larger two-way travel-time interval to generate the Fig. 3(c) GPR amplitude map. Pipe 2 on Fig. 3(d) provides a good example of strong upper and lower reflection hyperbola responses. A water-filled Pipe 2, however, did not exhibit a dual reflection hyperbola response on all the south-to-north GPR profiles. Conversely, although Pipe 1 and Pipe 4 each display one distinct reflection hyperbola response in Fig. 3(d), they often exhibited dual reflection hyperbola responses on other south-to-north GPR profiles representing undrained, extremely wet conditions. Furthermore, where a dual reflection hyperbola drainage pipe response is obtained, the lower response is typically stronger than the upper response. A detailed discussion of why dual reflection hyperbola responses were in many instances obtained for Pipes 1, 2, and 4 under undrained, extremely wet conditions is provided later with the GPR computer modeling results.

The soil-filled drain line (Pipe 3), however, always exhibited a single clearly distinguishable reflection hyperbola response on all south-to-north GPR profiles. As is exemplified by comparing Fig. 3(b) to Fig. 3(d), the Pipe 3 reflection hyperbola response is similar for both shallow hydrologic conditions tested. Hence, given a wet soil profile, the GPR reflection hyperbola response of a soil-filled drainage pipe is not greatly affected by whether the water table is above or below the drain line. Pipe A and Pipe B, in a manner similar to Pipe 3, always exhibited a single reflection hyperbola response, regardless of the shallow hydrologic conditions present, possibly indicating that these are nonfunctional drain lines that have become substantially filled with soil. It was somewhat puzzling as to why the soil-filled drain line produced a GPR response under any circumstance. The GPR computer modeling results discussed later provide an explanation as to why GPR was able to detect a soil-filled drain line.

Given just such a series of GPR profiles (measurement transects essentially perpendicular to drain line orientation) and suitable shallow hydrologic conditions, a water flow obstruction would be indicated at some point on the drain line if up-gradient of this point the drainage pipe was represented by strong upper and lower reflection hyperbolas, and down-gradient of this point the drainage pipe was represented by a single distinct reflection hyperbola. A potential problem arising with the use of GPR profiles oriented perpendicular to a drain line occurs when the water-filled pipe GPR response exhibits only one clearly distinguishable reflection hyperbola instead of two, as shown for Pipes 1 and 4 in Fig. 3(d), making it difficult to distinguish from the single distinct reflection hyperbola GPR response of an air-filled pipe. Furthermore, a very large number of closely spaced GPR measurement transects oriented perpendicular to a drain line would be required to find the precise location of an isolated crushed/severed pipe water flow obstruction. Determining the water conveyance functionality of a drain line using only GPR profiles that are oriented perpendicular to the drain line could therefore be somewhat impractical because of the large data collection effort required.

If map coordinates for locations along a drain line are available and suitable shallow hydrologic conditions exist, the best way for evaluating drain line conditions with respect to water conveyance functionality might be to collect GPR measurements along a transect that follows over top and along trend of the drain line from its beginning to its end. The drainage pipe response exhibited on a GPR profile generated from these measurements is that of a mostly flat-lying, banded linear feature (Figs. 4, 5, 6, and 7). Drain line depth variations shown on the GPR profiles along trend of a drain line (Figs. 4, 5, 6, and 7) are likely the result of attempts during installation to keep a uniform drain line slope from west to east even though there were minor irregularities in surface slope from west to east across the test plot. Drain line settling could also account for drain line depth variations observed in these GPR profiles. The GPR profile along Pipe 1 shown in Fig. 4(a) is an example of the banded linear GPR pipe response for drained (air-filled pipe), moderately wet shallow hydrologic conditions. The banded linear response, under undrained, extremely wet conditions along the unobstructed water-filled Pipe 1 is shown in Fig. 4(b). A comparison of Fig. 4(a) to Fig. 4(b) shows that, for GPR profiles oriented along trend of a drain line, the banded linear response is much stronger with an air-filled drainage pipe than with a water-filled drainage pipe.

Figures 4(a) and 4(b) additionally indicate that, regardless of the shallow hydrologic conditions present, the clay tile portion of Pipe 1 had a GPR response generally similar to the GPR response of the corrugated plastic tubing (CPT) portion of Pipe 1. A comparison of GPR profiles from measurement transects perpendicular to Pipe 1 also showed very little difference in the reflection hyperbola GPR response between a clay tile pipe and a CPT pipe. Therefore, as shown in this study, the pipe material (clay tile or CPT) seems to have little impact on the overall GPR pipe response, which corresponds well to results obtained by Allred *et al.* (2005b).

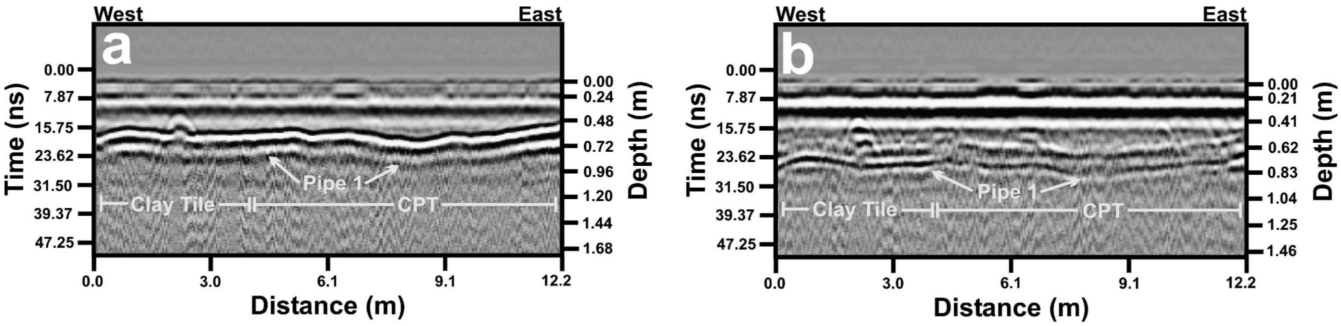

Figure 4. GPR profile along trend of Pipe 1: (a) drained, moderately wet conditions, air-filled pipe, and (b) undrained, extremely wet conditions, water-filled pipe.

Figure 5 shows three GPR profiles along trend of Pipe 2, which was the drain line having an isolated obstruction near its midpoint completely blocking the flow of water. Under drained, moderately wet conditions, an air-filled Pipe 2 (Fig. 5(a)) has a much stronger banded linear GPR response than the water-filled Pipe 2 (Fig. 5(b)) under undrained, extremely wet soil conditions. The Fig. 5(c) GPR profile along trend of Pipe 2 was obtained with an undrained, extremely wet soil profile, while water was continuously pumped from the east end of the drain line. Given these conditions, the east side of the drain line down-gradient of the isolated obstruction became air-filled after it was emptied of water, while the west side of the drain line up-gradient of the obstruction remained water-filled. Pipe 2 in Fig. 5(c) thereby mimicked conditions that often occur in a completely obstructed drain line during wet seasonal periods shortly after a significant rainfall event; a scenario that results in a water-filled pipe up-gradient of the obstruction and an air-filled pipe down-gradient of the obstruction. The location of the isolated obstruction near the midpoint of Pipe 2 is clearly indicated in Fig. 5(c) by the abrupt west-to-east transition from a weak water-filled pipe banded linear GPR response to a strong air-filled pipe banded linear GPR response. Consequently, Fig. 5(c) serves as an excellent example, based on suitable shallow hydrologic conditions, for using GPR profiles oriented along trend

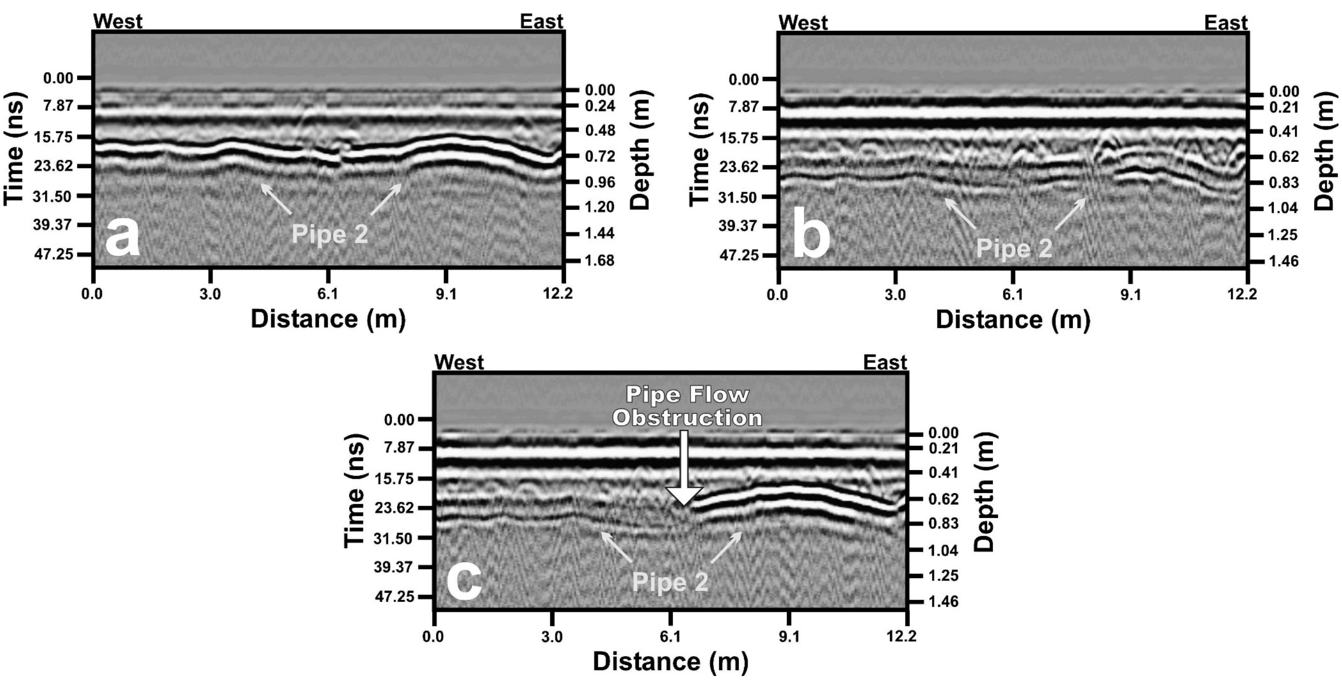

Figure 5. GPR profiles along trend of Pipe 2: (a) drained, moderately wet conditions, air-filled pipe, (b) undrained, extremely wet conditions, water-filled pipe, and (c) undrained, extremely wet conditions, water pumped and completely removed from the east side of the drain line.

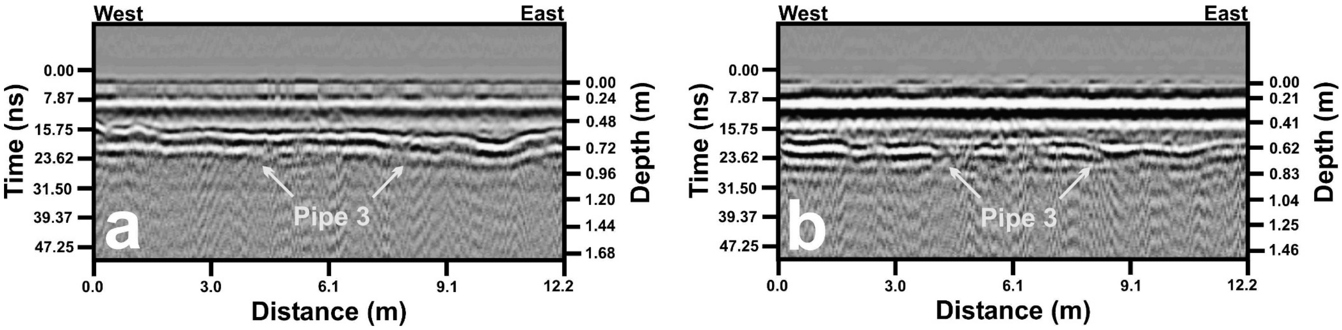

Figure 6. GPR profiles along trend of Pipe 3: (a) drained, moderately wet conditions, pipe contains unsaturated soil, and (b) undrained, extremely wet conditions, pipe contains saturated soil.

of the drain line to detect the potential presence of an isolated obstruction completely blocking the flow of water.

Figure 6 shows two GPR profiles along trend of Pipe 3, which itself was filled with soil. The banded linear response for Pipe 3 was relatively strong under both shallow hydrologic conditions tested. Close inspection of Figs. 6(a) and 6(b) does reveal the banded linear response for Pipe 3 under drained, moderately wet conditions (unsaturated soil-filled pipe) was slightly stronger and certainly more continuous than under undrained, extremely wet conditions (saturated soil-filled pipe). The GPR computer modeling results discussed later provide insight into the GPR responses obtained for the soil-filled drain line.

Figure 7 shows three GPR profiles along trend of Pipe 4, which was the drain line having a severed pipe partial flow obstruction near its midpoint. Under drained, moderately wet conditions, an air-filled Pipe 4 (Fig. 7(a)) has a stronger banded linear GPR response than the water-filled Pipe 4 (Fig. 7(b)) under undrained, extremely wet soil conditions. The Fig. 7(c) GPR profile along trend of Pipe 4 was obtained with an undrained, extremely wet soil profile, while water was continuously pumped from the east end of the drain line. Figure 7(c) shows a gradual transition from a strong banded linear GPR response along the western portion of the drain line to a weak banded linear response along the eastern portion of the drain line. The gradual transition in the Pipe 4 banded linear GPR response shown in Fig. 7(c)

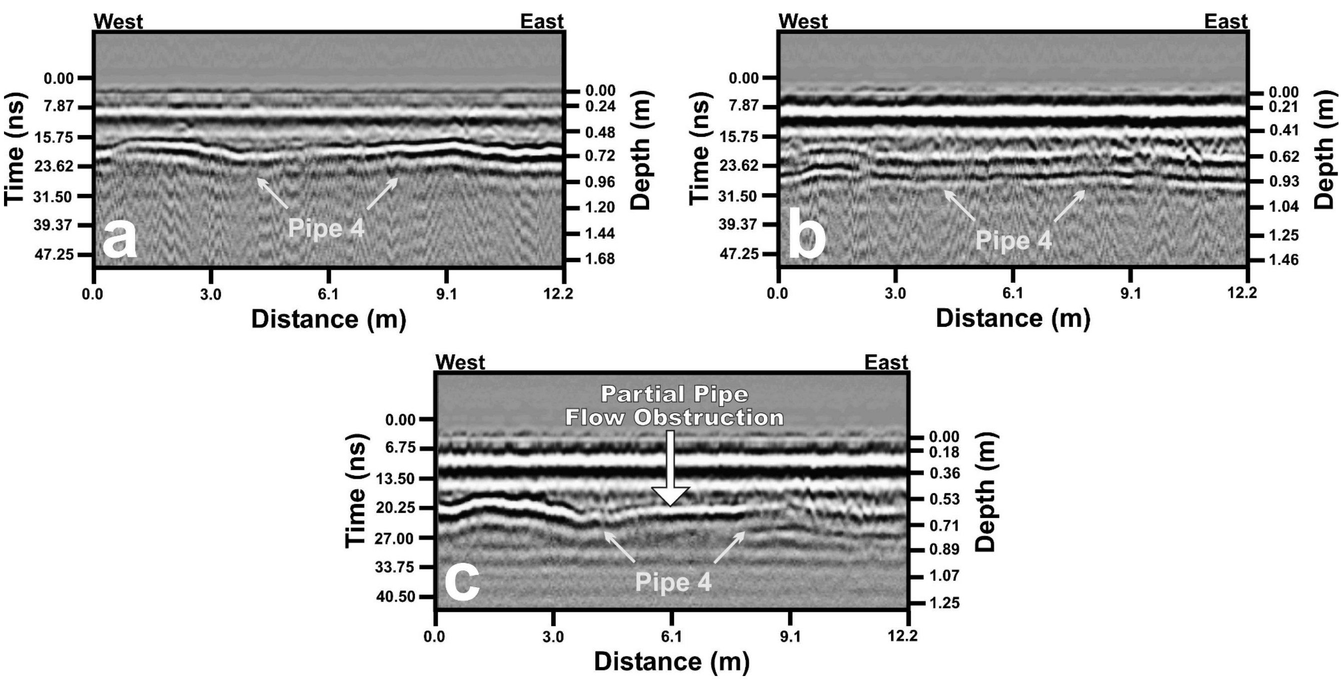

Figure 7. GPR profiles along trend of Pipe 4: (a) drained, moderately wet conditions, air-filled pipe, (b) undrained, extremely wet conditions, water-filled pipe, and (c) undrained, extremely wet conditions, water pumped from east end of drain line.

provides no clue as to the actual location of the severed drainage pipe partial obstruction. This result indicates there is still sufficient flow through the severed pipe partial obstruction for pumping at the east end of the drain line to cause the up-gradient, higher elevation western portions of the drain line to empty of water first and became air-filled (strong GPR response), while the down-gradient, lower elevation east side of the drain line still remained water-filled (weak GPR response). Consequently, the overall banded linear response shown in Fig. 7(c) indicates that Pipe 4 has maintained its water conveyance functionality, even with a partial flow obstruction present. It is worth noting that the GPR response shown in Fig. 7(c) is similar to the GPR response that would be obtained for a very specific subsurface drainage system scenario during a wet period of the year, shortly after a large rainfall event, given a properly functioning drain line, and within the very limited timeframe that the up-gradient, higher elevation portions of a drain line have had time to empty of water first, while the down-gradient, lower elevation portions of the drain line are still filled with water.

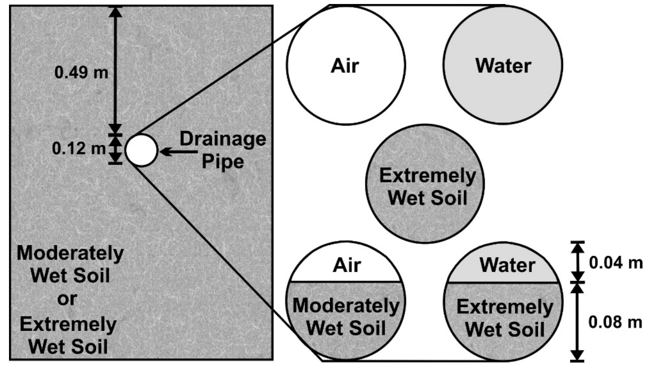

Figure 8. GPR drainage pipe response scenarios simulated with three dimensional computer software (GprMax3D): moderately wet soil outside a pipe completely filled with air; extremely wet (saturated) soil outside a pipe completely filled with air; extremely wet soil outside a pipe completely filled with water; extremely wet soil outside a pipe completely filled with extremely wet soil; moderately wet soil outside the pipe with air filling the top third of the pipe and moderately wet soil filling the bottom two thirds of the pipe; and extremely wet soil outside the pipe with water filling the top third of the pipe and extremely wet soil filling the bottom two thirds of the pipe.

Ground Penetrating Radar Computer Modeling

Synthetic GPR profiles were generated with the computer modeling software, GprMax3D, to assist with interpretation of GPR profiles produced from data collected at the field test plot. As depicted in Fig. 8, the GPR drainage pipe response was simulated for scenarios that include: moderately wet soil outside a pipe completely filled with air, extremely wet (saturated) soil outside a pipe completely filled with air, extremely wet soil outside a pipe completely filled with water, extremely wet soil outside a pipe completely filled with extremely wet soil, moderately wet soil outside the pipe with air filling the top third of the pipe and moderately wet soil filling the bottom two thirds of the pipe, and extremely wet soil outside the pipe with water filling the top third of the pipe and extremely wet soil filling the bottom two thirds of the pipe. The scenario with moderately wet soil surrounding a pipe completely filled with moderately wet soil was not simulated, because this particular scenario was expected to have a GPR response similar to the scenario already simulated for an extremely wet soil surrounding a pipe completely filled with extremely wet soil. GprMax3D required input of EC_a and relative dielectric permittivity values for materials outside and inside the drainage pipe. These input values are listed in Table 2 and were obtained from literature sources and test plot measurements (see Table 1).

The synthetic GPR profiles in Fig. 9, based on a measurement transect oriented perpendicular to the drain line and antennas parallel to the drain line, show the GPR drainage pipe response for five scenarios with different combinations of material outside the pipe (moderately wet soil or extremely wet saturated soil) and inside the pipe (air, water, moderately wet soil, or extremely wet saturated soil). The synthetic GPR profiles in Fig. 10, based on a measurement transect oriented along trend of a drain line and antennas perpendicular to the drain line, show the GPR drainage pipe response for five scenarios with different combinations of material outside and inside the pipe. The synthetic GPR drainage pipe responses depicted in the Fig. 9 and 10 profiles show strong similarity in most cases to the actual test plot GPR drainage pipe responses shown in the Figs. 3, 4, 5, 6, and 7 profiles.

As was generally found with the field data (see Figs. 3(b) and 3(d)), computer modeling indicates that, for a measurement transect perpendicular to the drain line, the drainage pipe response shown on a GPR profile will be a single reflection hyperbola given drained (air-filled pipe), moderately wet soil conditions (Fig. 9(a)), while under undrained (water-filled pipe), extremely wet soil conditions, the response will be a dual upper and lower reflection hyperbola (Fig. 9(c)). The reason why a single reflection hyperbola response is obtained with an air-filled pipe and a dual reflection hyperbola response is obtained with a water-filled pipe is best explained by first considering the fact that radar waves pass from the side of the drainage pipe closest to the GPR antennas, through an air/water/soil-filled interior, to the other side

Table 2. Relative dielectric permittivity and apparent soil electrical conductivity (EC_a) values input into GprMax3D.

	Materials outside of pipe		Materials inside of pipe			
	Moderately wet soil	Extremely wet saturated soil	Air	Water	Moderately wet soil	Extremely wet saturated soil
EC_a (mS/m)	14.7	17.7	0.0	10.0	14.7	17.7
Relative dielectric permittivity	19.7	25.4	1.0	83.7	19.7	25.4

of the drainage pipe furthest from the GPR antennas, in turn producing reflected radar signals from both sides of the pipe. If the radar signals reflected from both sides of the pipe are strong and there is sufficient separation in their arrival time at the receiving antenna, then an upper and lower reflection hyperbola response should be anticipated. When only air is present inside the pipe, the radar wave velocity through the pipe interior is fast enough that there is very little time separation between the radar signals reflected from both sides of the pipe, and in actuality, the time separation between the two reflected radar signals is so small that the two signals become superimposed on one another, thereby producing a single reflection hyperbola as shown in Fig. 9(a). For the same reason, pipes filled with an air/soil combination, or a water/soil combination will also likely produce what appears to be a single reflection hyperbola response (Figs. 9(b) and 9(d)). Conversely, when water completely fills the inside of the pipe, the radar wave velocity through the pipe interior is slow enough that there is sufficient time separation between the radar signals reflected from both sides of the pipe such that there is no interference between the two reflected radar signals, resulting in a dual reflection hyperbola response as shown in Fig. 9(c). Zeng and McMechan (1997) obtained GPR modeling results for an air- or water-filled, 16-cm diameter, thin-walled, PVC plastic pipe that were similar, respectively, to those presented in Figs. 9(a) and 9(c). Additionally, Fig. 9(c) also shows that, for a dual upper and lower reflection hyperbola response, the lower reflection hyperbola is stronger, which is a finding often observed with the GPR data collected at the test plot (see Pipe 2 in Fig. 3(d)). This result may be caused by a radar energy focusing effect that occurs when a radar signal passes from lower relative dielectric permittivity material to a higher relative dielectric permittivity material (Conyers and Goodman, 1997), such as the case when the radar signal

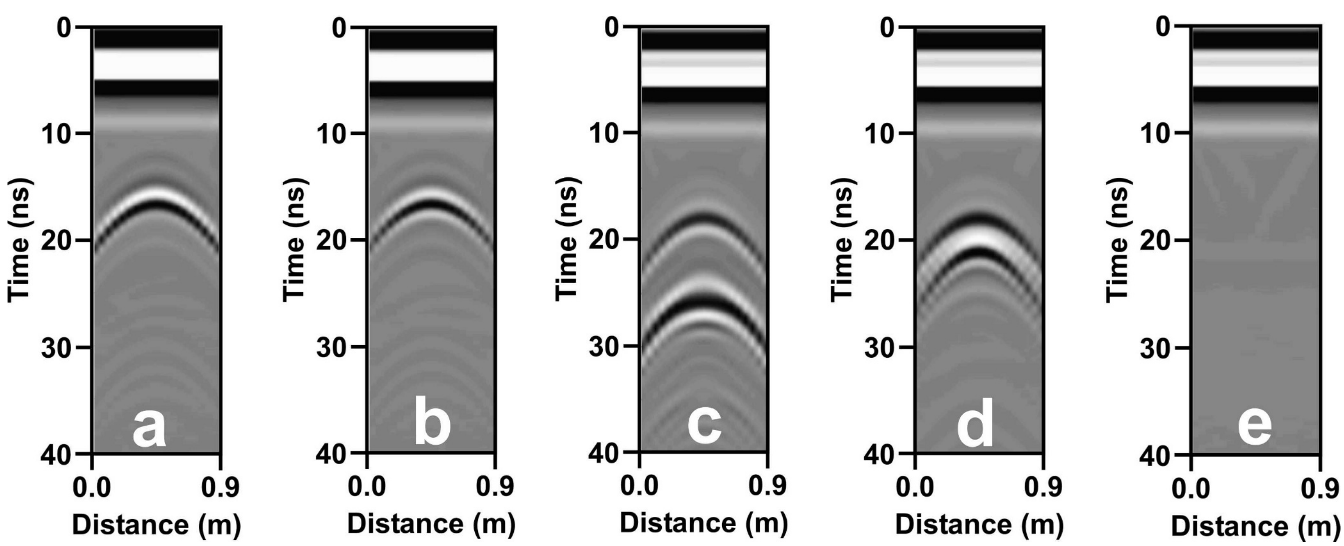

Figure 9. Synthetic GPR profiles from computer modeling with antennas oriented perpendicular to the measurement transect and parallel to the drain line: (a) moderately wet soil outside of pipe and air inside of pipe, (b) moderately wet soil outside of pipe while inside of pipe the bottom 2/3 is filled with moderately wet soil and the top 1/3 is filled with air, (c) extremely wet soil outside of pipe and water inside of pipe, (d) extremely wet soil outside of pipe while inside of pipe the bottom 2/3 is filled with extremely wet soil and the top 1/3 is filled with water, and (e) extremely wet soil outside of pipe and extremely wet soil inside of pipe.

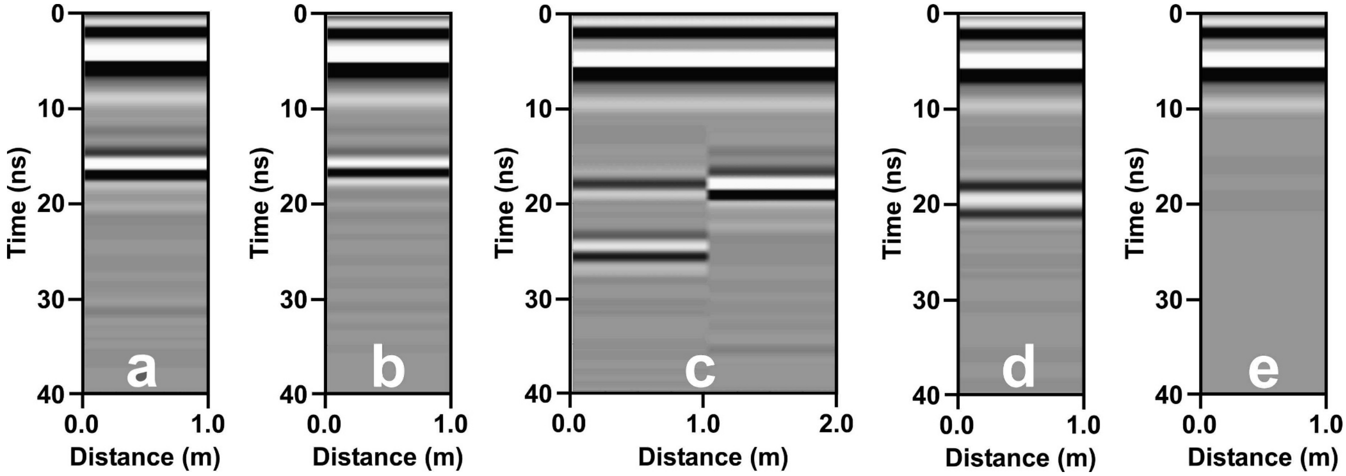

Figure 10. Synthetic GPR profiles from computer modeling with antennas oriented perpendicular to measurement transect and perpendicular to drain line: (a) moderately wet soil outside of pipe and air inside of pipe, (b) moderately wet soil outside of pipe while inside of pipe the bottom 2/3 is filled with moderately wet soil and the top 1/3 is filled with air, (c) extremely wet soil outside of pipe while inside of pipe is water-filled from a distance of 0.0 to 1.0 m and air-filled from a distance of 1.0 to 2.0 m, (d) extremely wet soil outside of pipe while inside of pipe the bottom 2/3 is filled with extremely wet soil and the top 1/3 is filled with water, and (e) extremely wet soil outside of pipe and extremely wet soil inside of pipe.

passes from the soil outside the pipe (relative dielectric permittivity = 25.4) to the water inside the pipe (relative dielectric permittivity = 83.7).

Figures 9(e) and 10(e) indicate that there is no GPR drainage pipe response for a completely soil-filled pipe, if the water content conditions for the soil inside the pipe are the same as the water content conditions for soil outside the pipe. However, drainage pipes that are partially filled with soil do produce a GPR response as is depicted in Figs. 9(b), 9(d), 10(b), and 10(d). Consequently, since GPR responses were obtained for the soil-filled pipe at the test plot (see Figs. 3(b), 3(d), and 6), the pipe itself was in all likelihood not completely soil-filled, but rather only partially soil-filled (same as the Fig. 1 example). In this research, a partially soil-filled pipe probably resulted from settlement of the soil packed inside the pipe, and this settlement undoubtedly occurred over time after the drain line was originally installed at the test plot. Finally, along with Fig. 5(c), the Fig. 10(c) synthetic GPR profile strongly supports the potential of GPR data collection along trend of a drain line as a means to pinpoint a complete water flow obstruction, given the right hydrologic conditions.

General Considerations Regarding Shallow Hydrologic Conditions and Ground Penetrating Radar Assessment of Drainage Pipe Water Conveyance Functionality

This investigation confirms that GPR can be employed to locate pipes under drained, moderately wet and undrained, extremely wet soil conditions. Previous research also indicates that GPR can detect pipes in dry soils (Allred *et al.*, 2005b). Both the test plot GPR data collection and GPR computer modeling components of the study clearly show that GPR response differences between air-filled and water-filled drainage pipes make it possible for GPR to provide insight on potential drainage pipe water conveyance problems. However, for GPR discovery of drainage pipe water conveyance functionality problems, certain shallow hydrologic conditions are needed which produce a water-filled drain line up-gradient of a pipe flow obstruction and an air-filled drain line down-gradient of the a pipe flow obstruction. Wet periods of the year (late fall, winter, and early spring), a couple of days after significant rainfall event, are likely to produce this type of scenario in which GPR can be employed to isolate pipe flow obstructions. Ground penetrating radar is unlikely to provide any insight on pipe flow obstructions for situations with very dry soils and completely air-filled drain lines or saturated soils with completely water-filled drain lines. Future research will focus on evaluating GPR soil water content mapping (Grote *et al.*, 2003; Huisman *et al.*, 2003) as a possible means of assessing potential subsurface drainage system problems, because wet soil spatial anomalies may indicate field locations where drainage pipes are not functioning properly.

Summary and Conclusions

Ground penetrating radar (GPR) surveys using 250 MHz transmitter/receiver antennas were conducted at a specially designed test plot for the purpose of confirming GPR drainage pipe detection capabilities, and then determining whether GPR can provide useful insight into drain line water conveyance functionality. The test plot contained four drain lines: one open to flow and comprised of clay tile along part of its length with the rest constructed of corrugated plastic tubing (CPT); one comprised of CPT with an isolated obstruction near the midpoint, completely preventing through-flow of water; one comprised of CPT but filled with soil; and one comprised of CPT but severed near its midpoint, producing a partial obstruction to water flow. Ground penetrating radar data were collected at the test plot under drained, moderately wet soil conditions (water table below drain lines) and undrained, extremely wet soil conditions (water table above drain lines). Ground penetrating radar computer modeling simulations were conducted to assist with the interpretation of the GPR data collected at the field test plot. The major findings of the investigation are listed as follows:

1) Under drained, moderately wet and undrained, extremely wet shallow hydrologic conditions, GPR proved capable of mapping drain lines buried to a depth of 0.6 m in a clay loam soil.
2) Given the proper conditions regarding shallow hydrology, GPR data collected along trend of a drain line can be used to precisely locate an isolated obstruction that completely blocks the flow of water through the drain line.
3) An isolated partial obstruction that does not completely block the flow of water through the drain line will be difficult to locate with GPR.
4) Ground penetrating radar computer modeling indicates that a partially soil-filled drainage pipe produces a response shown on GPR profiles that in most cases will be difficult to distinguish from the GPR profile response of a pipe which contains no soil. However, based on test plot GPR data, relatively weak drain line responses depicted on a GPR amplitude map may be indicative of a drainage pipe that is partially soil-filled.
5) Ground penetrating radar computer modeling can be an important tool for interpreting GPR field data collected for assessing drainage pipe conditions.

Consequently, the findings of this research support the feasibility of using GPR to not only locate buried agricultural drainage pipes, but to also, given the right field conditions, determine drain line conditions regarding ability to deliver water. Future research will focus on GPR soil water content mapping as a potential method for delineating parts of an agricultural field where the subsurface drainage pipe system is not functioning properly.

Acknowledgments

The authors would like to express their appreciation to Phil Levison and Sarah Boone for their help with installing drainage pipe at the test plot. Dedra Woner conducted the particle size analysis on the test plot soil samples.

References

Allred, B.J., Fausey, N.R., Peters Jr., L., Chen, C., Daniels, J.J., and Youn, H., 2004, Detection of buried agricultural drainage pipe with geophysical methods: Applied Engineering in Agriculture, **20**, 307–318.

Allred, B.J., Redman, J.D., McCoy, E.L., and Taylor, R.S., 2005a, Golf course applications of near-surface geophysical methods: A case study: Journal of Environmental and Engineering Geophysics, **10**, 1–19.

Allred, B.J., Daniels, J.J., Fausey, N.R., Chen, C., Peters Jr., L., and Youn, H., 2005b, Important considerations for locating buried agricultural drainage pipe using ground penetrating radar: Applied Engineering in Agriculture, **21**, 71–87.

Boniak, R., Chong, S.K., Indorante, S.J., and Doolittle, J.A., 2002, Mapping golf course green drainage systems and subsurface features using ground penetrating radar *in* Proceedings of SPIE, Vol. 4758, Koppenjan, S.K., and Lee, H. (eds.), Ninth International Conference on Ground Penetrating Radar, International Society of Optical Engineering, 477–481.

Chow, T.L., and Rees, H.W., 1989, Identification of subsurface drain locations with ground-penetrating radar: Canadian Journal of Soil Science, **69**, 223–234.

Conyers, L.B., and Goodman, D., 1997. Ground-penetrating radar: An introduction for archaeologists, AltaMira Press, Walnut Creek, California.

Conyers, L.B., 2004. Ground-penetrating radar for archaeology: AltaMira Press, Walnut Creek, California.

Giannopoulos, A., 2009, GprMax: A ground penetrating radar simulation tool http://www.gprmax.org.

Grote, K., Hubbard, S., and Rubin, Y., 2003, Field-scale estimation of volumetric water content using ground-penetrating radar ground wave techniques: Water Resources Research, **39**, 1321–1333.

Hayakawa, H., and Kawanaka, A., 1998, Radar imaging of underground pipes by automated estimation of velocity distribution versus depth: J. Applied Geophysics, **40**, 37–48.

Huisman, J.A., Hubbard, S.S., Redman, J.D., and Annan, A.P., 2003, Measuring soil water content with ground penetrating radar: A review: Vadose Zone J., **2**, 476–490.

LaFaleche, P.T., Todoeschuck, J.P., Jensen, O.G., and Judge, A.S., 1991, Analysis of ground probing radar data: Predictive deconvolution: Canadian Geotechnical J., **28**, 134–139.

Pavelis, G.A., 1987, Economic survey of farm drainage *in* Farm drainage in the United States: History, status, and prospects, Miscellaneous Publication Number 1455, Pavelis, G.A. (ed.), U.S. Dept. of Agriculture, Economic Research Service, 110–136.

Peters Jr., L., and Young, J.D., 1986, Applications of subsurface transient radar *in* Time domain measurements in electromagnetics, Miller, E.K. (ed.), Van Nostrand Reinhold, New York, New York, 297–351.

Sensors & Software Inc., Ekko_View Enhanced and Ekko_View Deluxe user's guide, Sensors & Software, Inc., Mississauga, Ontario, Canada.

Sutinen, R., 1992. Glacial deposits, their electrical properties and surveying by image interpretation and ground penetrating radar, Bulletin 359, Geological Survey of Finland, Rovaniemi, Finland.

Wensink, W.A., Hofman, J., and Van Deen, J.K., 1991, Measured reflection strengths of underwater pipes irradiated by pulsed horizontal dipole in air: Comparison with continuous plane-wave scattering theory: Geophysical Prospecting, **39**, 543–566.

Wray, W.K., 1986. Measuring engineering properties of soil: Prentice-Hall, Inc., Englewood Cliffs, New Jersey.

Zeng, X., and McMechan, G.A., 1997, GPR characterization of buried tanks and pipes: Geophysics, **62**, 797–806.